Dispersion Modelling Studies:
the 1984 Experiment in Angra dos Reis

P. Martano[1], A.S. Paschoa[2]

[1] *CNR ISIAtA, Via Monteroni, 73 100 Lecce, ltalia*

[2] *Pontifícia Universidade Católica do Rio de Janeiro (PUC-Rio),*

Depto, de Física, C. P. 38071, Rio de Janeiro, RJ 22452-970, Brasil

The results of a numerical modelling of an atmospheric dispersion campaign in Angra dos Reis (R.J., Brazil) are considered. A comparison between model results and monitored field concentrations is discussed from the point of view of its statistical as well as physical significance. Particular attention has been paid to the effects of the lack of homogeneity in the atmospheric fields both in the spatial scale (horizontal and vertical) and in the time scale (stationarity in the local meteorology), as they can be critical in coastal areas. Some suggestions are made about a real time modelling of the atmospheric dispersion on the considered site.

Neste trabalho são revistos os resultados de uma modelagem anterior de um experimento de dispersão atmosférica realizado em Angra dos Reis, RJ, Brasil. Discute-se o significado estatístico e físico da comparação entre os resultados obtidos através do modelo e aqueles de concentrações medidas por meio de amostragem de campo. Foi dada atenção particular aos efeitos decorrentes da falta de homogeneidade dos campos atmosféricos, tanto em termos de escala espacial (horizontal e vertical), quanto de escala temporal (estacionariedade da meteorologia local), por serem ambas criticas nas áreas costeiras. Inferiu-se algumas indicações sobre a modelagem em tempo real da dispersão atmosférica no local considerado.

I. Introduction

Two difficult problems must be faced in modelling atmospheric dispersion in coastal sites with a complex topography, even in short time/space scale simulations (i,e.: order of hours and tens of kilometres in the horizontal respectively). Modelling:

1) The atmospheric flow and turbulence over a changing surface, in particular when the available meteorological data have a much lower spatial resolution than the desired modelling scale and/or the scale of the topographic features. This means modelling the mechanical distortion of the flow and the turbulence as well as the vertical stratification of the boundary layer, both of which are strongly sensitive to the horizontal inhomogeneities of the underlying surfaces: a problem of spatial short scale variability.

2) Now taking into account the effects of the small-scale time variability due to the thermal forcing induced by the temperature differences in the underlying surfaces (i.e. ground and water). This means modelling facing the short-term variability associated with the thermally-driven local-scale circulations.

Considering the first problem, the most used approaches for a windfield reconstruction over a complex topography are (Lalas-Ratto, 1996) [1]:

i) the mass-consistent one, basically an interpolation of wind data with a zero-divergence constraint over the flow field, imposed by Sasaki's (1958) [2] method

ii) the calculation of the windfield by the dynamical momentum equations, generally based on the linearised approach of the early work of Jackson and Hunt (1975) [3], and subsequent developments.

Both methods have some shortcomings: the former needing a good resolution on the initial data set to be able to get a reasonable approximation of the windfield

on the required spatial scale, and the latter limited by the linearised approach to a gentle-sloped topography. Then, a proper reconstruction of the windfield can be difficult when both these conditions do not hold.

The other aspect related to the spatial inhomogeneity is the change in the boundary layer vertical structure associated to the temperature differences in the underlying surfaces.

The formation of a Thermal Internal Boundary Layer (TIBL) for onshore wind conditions across a coastline has been extensively studied. Raynor et al., (1975) [4] and Lyons, (1976) [5], pointed out its effects on atmospheric dispersion and approximately estimated its vertical development onshore from the coastline. Their results suggest that the developing vertical structures in the boundary layer are very effective in determining the dispersion in coastal areas and should be kept thoroughly into account in the model simulations.

Actually, inhomogeneities of the surface conditions involve also changes in roughness and humidity conditions. Studies of their effect on the micrometeorology of the lower boundary layer can be found for example in the book by Brutsaert (Brutsaert, 1982) [6], but they are generally believed to be less effective in changing the dispersion properties of the atmospheric boundary layer than the thermal inhomogeneities in conditions of strong insolation. Anyway, that problem involves a lot of different aspects that can usually hardly faced altogether. They are related to the thermally induced mesoscale components in the flow fields and associated short term meteorological variability (Atkinson, 1981) [7]. Martano (1996a) [8] showed that about 50 per cent of the total surface wind speed variability is accounted by thermally induced mesoscale circulations at a midlatitude coastal site. This percentile is expected to be even increased in tropical regions, where the diurnal mesoscale variability is often the dominant meteorological component (Hastenrath, 1991) [9]. The main effects are not only the recirculations associated to the formation of well-developed density currents (sea/land breezes, whose horizontal extension defines the coastal zone), but in general the small scale

atmospheric disturbances that can act in feedback with the heating/cooling of the water surface associated to sea currents/tides. This interplay between atmospheric and surface water dynamics can generate a scenario of very short-term variability of the local meteorological conditions that is typical of the coastal zone and can cause difficulties in both modelling dispersion and comparing model results with experimental data.

As pointed out by Martano (1996b) [10], these difficulties are related to the non-stationarity of the local meteorological conditions that govern the turbulent diffusivity field, which can have two main consequences. a) In these conditions it could be a poor approximation to use a static reconstructed windfield for the whole simulation time of the dispersion (for example the time T in which the field concentration samples have been averaged). In other words: the meteorological conditions could show significant time trends in time scale of the order of the simulation time.

b) The stationarity time scale T_s (the shortest time lag after which the local meteorological variables show significant time trends) and the correlation time T_c of the concentration fluctuations could not be so well-separated (orders of magnitude), as required for a thorough application of a statistical analysis in comparing the model dispersion results and the sampled concentration time averages. In other words: the inequality $T_c << T << T_s$, that is required in any statistically meaningful analysis, could not be sufficiently verified. Actually many of the above aspects appeared as relevant in modelling the 1984 dispersion experiment in Angra dos Reis (RJ, Brazil). They are focused in the following sections and discussed in connection with the simulation results.

2. The dispersion experiment

The dispersion experiment is described in Biagio et al. (1985) [11].

The site of Itaorna Beach (Angra dos Reis, RJ) is shown in Fig. 1, along with the location of the measurement sites (numbered).
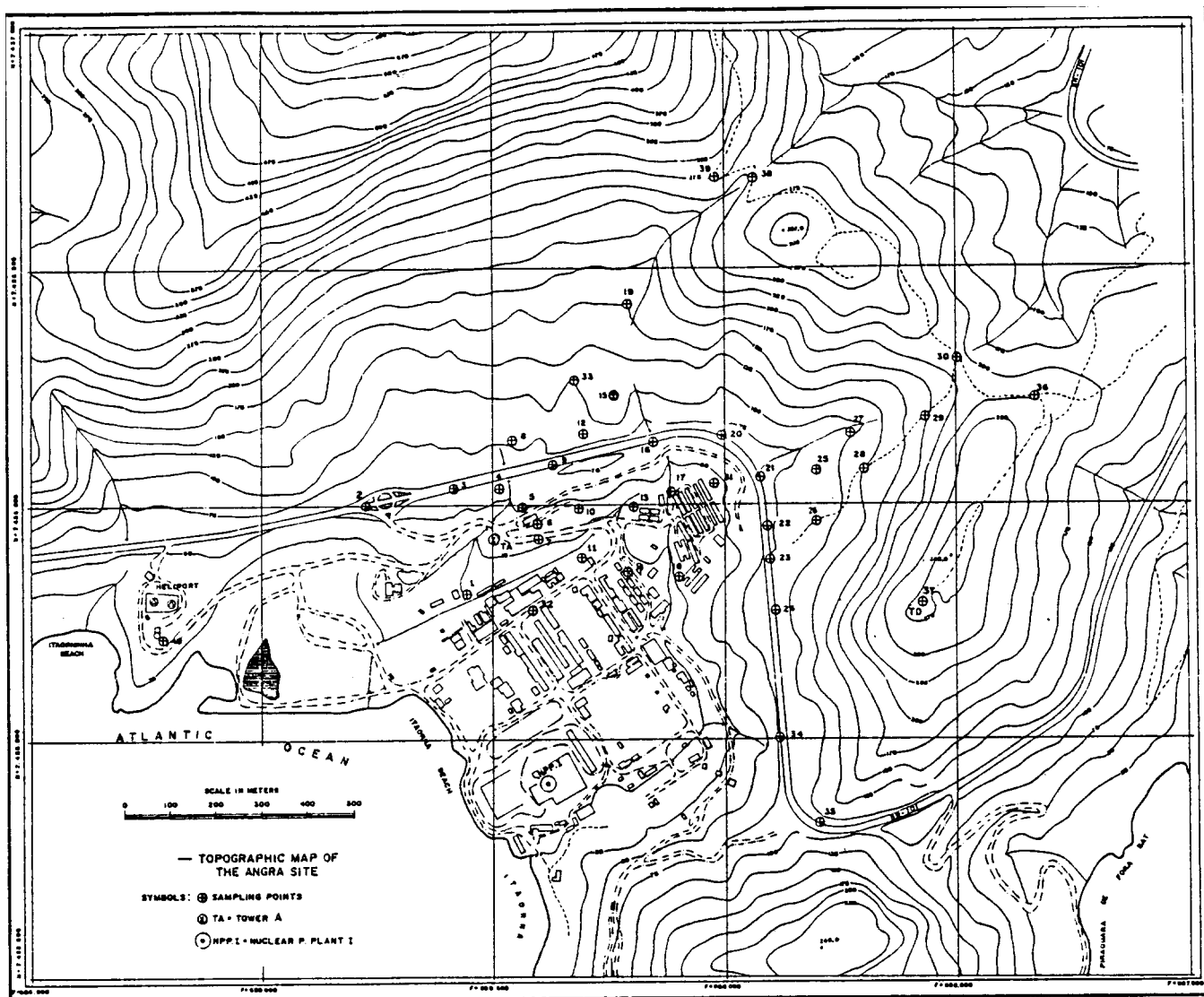
Figure 1. Map ofthe experiment site (from Biagio et al., 1985) [11]. The numbered locations indicate the monitored concentration points.

The experiment consisted in the controlled releases of tritiated water vapour from the meteorological tower TA, 100 m height, close to the power plant in Itaorna Beach, dunng five days from 28 November to 4 December 1984. The total time of emission was of 90 minutes for each day, always around midday LST. The collection of water vapour over cooled aluminium plates in the numbered location in the figure took place in three subsequent periods of 20 minutes each, 30 minutes after the beginning of the release, to allow the source and the plume transport to reach a supposed stationary condition on the measurement area (say, after reaching the monitoring area for a time longer than the correlation time T_c).

During the whole experiment, four meteorological towers (TA,TB, TC, TD) collected the relevant meteorological data averaged over 15 minutes in the following way.

Wind speed and direction are measured at three levels on TA (10, 60 and 100 m), along with the temperature gradient between 10 and 100 m., and TB, TC and TD measured the wind speed at 15 m above the ground only.

Some additional data of relative humidity are available in some of the sampling sites, and are used to calculate the concentration of tritiated water in the air (after measuring the radioactivity of the collected samples). All relevant details, as well as the synoptic meteorolog-

ical conditions during the dispersion campaign are also described in Biagio et al. (1985) [11].

3. The experiment model

An attempt to model the dispersion experiment has already been made (Martano, 1992; Martano et al. 1991) [13,14] breaking the task into two steps:

1) Reconstruction of a (stationary) windfield in the dispersion area for each of the modelled experiments.

2) Applying a dispersion model over the obtained windfield with attention paid to the local dispersion characteristics of the atmospheric boundary layer.

3.1 Windfield reconstruction

The typical solution to a problem of windfield re-

construction in topographically complex sites where sparse experimental data are available is to use an interpolative mass-consistent model (Lalas-Ratto, 1996) [1]. This is possible by imposing the non-divergence condition over a zero-order approximation windfield (U_0, V_0, W_0), consisting of a simple mathematical interpolation of the experimental data on the site, to obtain a physically more reliable one in which mass is conserved.

Usually, the non-divergent approximation is obtained after a minimisation of Sasaki's functional I (Sasaki, 1958) [2], that is the field-averaged mean square error between final field (U,V,W) and 'zero-order' one, with the non-divergence constraint imposed, say:

$$I = \int a_h^2 [(U - U_0)^2 + (V - V_0)^2] + a_v^2 (W - W_0)^2 + \phi \left(\frac{\partial U}{\partial x} + \frac{\partial V}{\partial y} + \frac{\partial W}{\partial z} \right) dxdydz \qquad (3.1)$$

It is easy to show that a linear partial differential equation for ϕ can easily be obtained applying the variational principle along with appropriate boundary conditions to the equation (3.1), and using the continuity equation. After numerically solving the resulting differential equation, the non-divergent windfield can be obtained as:

$$U - U_0 = (1/2a_h)^2 \partial\phi/\partial x$$

$$V - V_0 = (1/2a_h)^2 \partial\phi/\partial y$$

$$W - W_0 = (1/2a_v)^2 \partial\phi/\partial z \qquad (3.2)$$

The ratio between the two parameters a_h and a_v determines the weight of the adjusting procedure related to the horizontal and vertical components respectively (Lalas-Ratto,1996)[1], and can be changed by the user taking into account the characteristics of the initial data and the atmospheric stability ($a_h = a_v = 1$ have been chosen in the described simulations, that should

be suitable for neutral and convective conditions, see also section 3.2).

The ATMOS1 model (Zanini-Busuoli, 1991a) [14], that was used in this simulation, is based on the previous approach, rewritten in conformal coordinates (x, y, σ) where:

$$\sigma = (z_t - z)/(z_t - z_s) = (z_t - z)/\delta \qquad (3.3)$$

Here, z_t is the height of the top and z_s the height of the bottom of the simulation domain, in a Cartesian reference frame.

The slight mathematical complication of the resulting equations is largely overcome by the advantages of using terrain-following co-ordinates. In fact is straightforward to impose the bottom boundary condition to the resulting flat surface $\sigma = 1$ of the bottom, and the expansion of the vertical resolution close to the ground (see eq.(3.3)) is useful in dispersion problems.

The result of this procedure remains strongly depending on the initial 'zero order' interpolated field, that means on the available experimental data set. The

latter is then required to be as detailed as possible on the given site, with data spacing less then, or comparable with, the typical horizontal scale of the orographical relief, to obtain results close to the actual windfield. The mass-consistent procedure is in fact unable to add information to the wind dynamics where it is lacking.

Then the scarcity of the available meteorological data set in describing the windfield over the complex topography of Itaorna Beach imposed additional information to be added to data set initialising the mass-consistent model, to increase the spatial resolution.

This was accomplished with the aid of the dynamical linearised model FLOWSTAR (Carruthers et al. 1988) [15], that enabled the numerical calculation of some additional vertical profiles of windspeed in suitable locations (ST1, ST2, ST3 in Fig.2a).The new information come from the solutions of the linearised equations of turbulent flux over topography (Hunt et al. 1988) [15], taking the available experimental profile in TA as reference to initialise the model, as described in detail by Martano (1992)[12].

In principle, the FLOWSTAR model, as any linearised one for turbulent flux over topography, is only suitable for use in front of gentle slopes, and so it cannot be useful for the reconstruction of the whole windfield on the site (Martano, 1992)[12]. Nevertheless the additional information added as approximated calculated profiles (in locations with gentle slope) could aid the mass-consistent model to get a final result closer to the actual windfield than that obtained using the only available experimental profile in TA. The selected locatlons, as well a their number, remain subjected at this stage to the sensible arbitrariness of the user's experience and skillness.

For each of the modelled experiments some different windfields were reconstructed applying the ATMOS 1 model respectively to only the experimental data set, only the reconstructed profiles set (in ST1, ST2 and ST3), and to both (all available information). An example of the three surface winfields are shown in Fig. 2a,b,c for the experiment number 4 (from: Martano, 1992)[12].
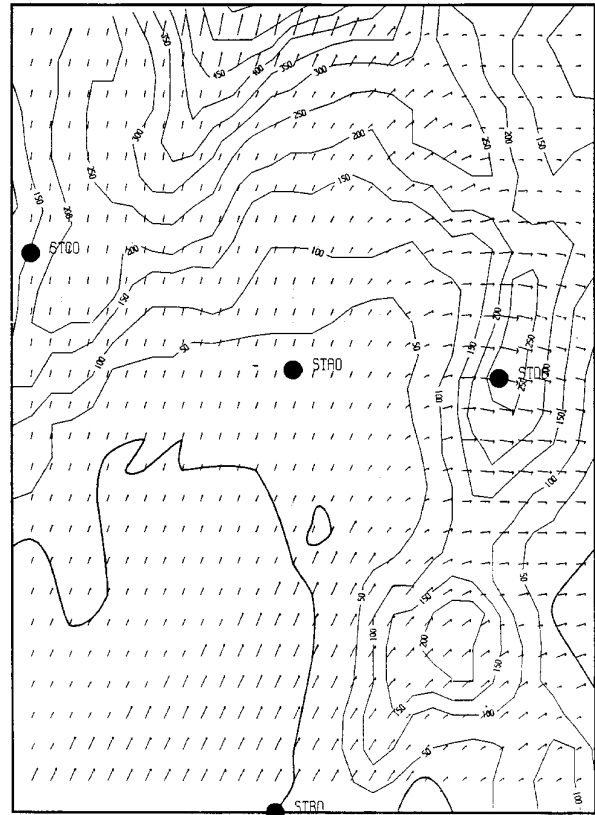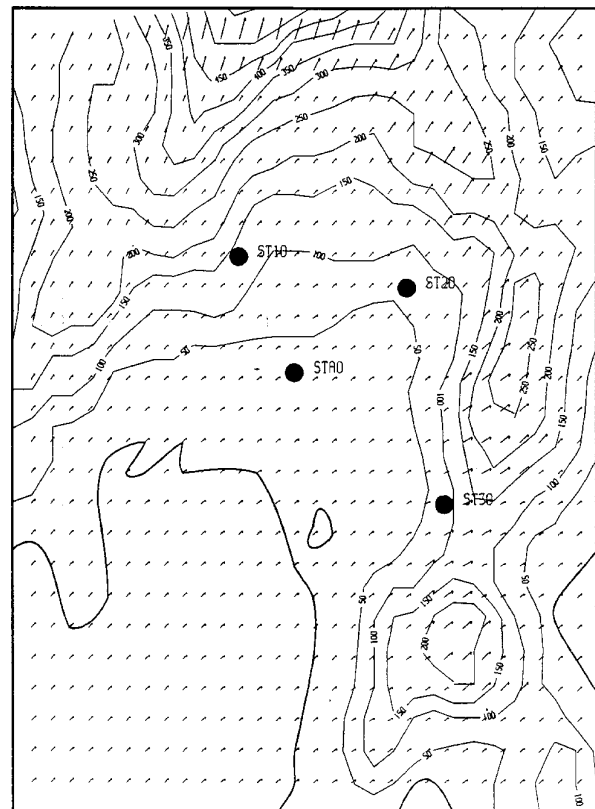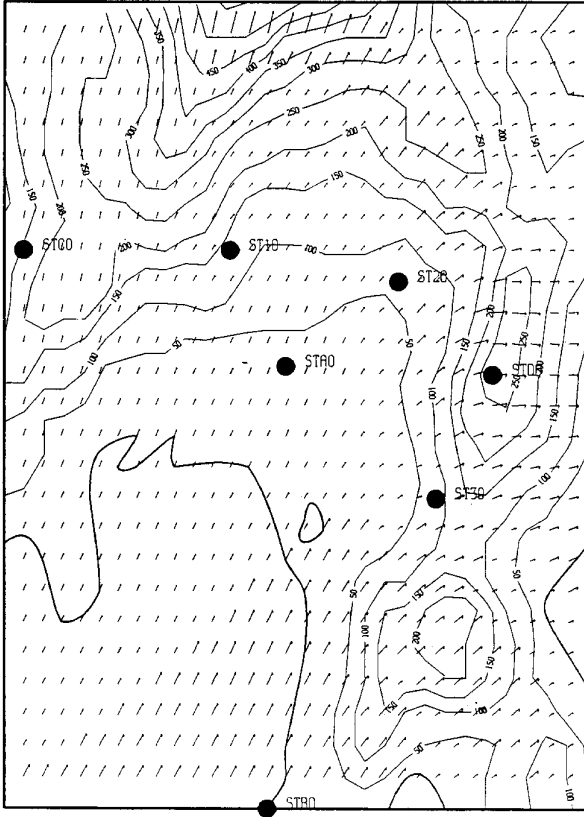

Figure 2a

Figure 2b

Figure 2c

Figure 2. Surface windfield for Exp4. Dots indicate the location of the used wind data. The coastline is represented by the thick line. The shape of the map is due to a standard graphic output of the model. a) Simulation with only experimental data. b) Simulation with only Flowstar data. c) All wind data simulation.

3.2 Dispersion calculations

The dispersion calculation was accomplished by numerically solving a the advection-diffusion equation over the calculated windfield, in the form of the ATMOS2 code (Busuoli-Zanini, 1991b)[17].

In conformal co-ordinates the advection-diffusion equation for the mean concentration C reads:

$$\frac{\partial(\delta C)}{\partial t} + \frac{\partial(\delta U C)}{\partial x} + \frac{\partial(\delta V C)}{\partial y} + \frac{\partial(\delta W'C)}{\partial \sigma} =$$

$$\frac{\partial}{\partial x}\left[\frac{K_x \partial C}{\partial x}\right] + \frac{\partial}{\partial y}\left[\frac{K_y \partial C}{\partial y}\right] + \frac{\partial}{\partial \sigma}\left[\frac{K_\sigma \partial C}{\partial \sigma}\right] + S \quad (3.4)$$

where

$$W' = \frac{1}{\delta}\left[\sigma U \frac{\partial z_s}{\partial x} + \sigma V \frac{\partial z_s}{\partial y} - W\right]$$

and K_x, K_y, K_z are the turbulent dispersion coefficients in Cartesian coordinates x, y, z respectively, $K_\sigma = K_z/\delta^2$ and S is the source term.

Here the dispersion coefficients (windfield dependent!) are calculated following a mixing length approach in the form of:

$$K_z = k\sigma_\alpha U_z l$$
$$K_y = \beta k\sigma_\alpha U_y l$$

$$K_x = \beta k\sigma_\alpha U_x l \quad (3.5)$$

where l is the mixing length, σ_α the angular standard deviation of the turbulent velocity, k the von Karman constant and β a stability dependent coefficient for the horizontal dispersion.

The wind velocity scales U_x, U_y, U_z, are 'first neighbours' grid averages of the windfield components around the point (x, y, z), calculated following the numerical algorithm of Smith and Howard (1972) [18], and the experimental values of l, σ_α and β are given as functions of height and stability class following Taylor et al. (1970) [19].

In this way the model allows a point-by-point estimation of the atmospheric stability conditions on the windfield grid, that was used to simulate a coastal TIBL.

In fact the dispersion simulations were accomplished on the windfield grids comparing two different stability schemes:

i) a uniform neutrality of ABL stability on the site (simply extending the only available suggestion from the thermal lapse rate measured in TA)

ii) A convective condition near the ground degrading to a neutral one at a typical TIBL height h_T, depending on the along-wind distance d from the coastline (that is increasing in some sense the vertical resolution of the stability information).

Taking into account the analysis of Stunder and Sethu Rarnan (1984)[20], the classical expression due to Raynor (Raynor et al. 1975)[4] was selected as a simplest effective evaluation of h_T for these practical purposes:

$$h_T = (u*/U_r)(d|T_a - T_w|\gamma)^{1/2} \quad (3.6)$$

where $u*$ (friction velocity) and U_r (average windspeed at $z=10$ m) were calculated from the obtained FLOWSTAR profiles, T_a and T_w are the surface air and sea temperatures, and the surface lapse rate γ was given an average value of $0.01°C/m$.

Some results of the dispersion simulation are shown in Fig 3.a,b,c for the surface concentration isopleths in EXP4, and corresponding to the above scheme ii) and

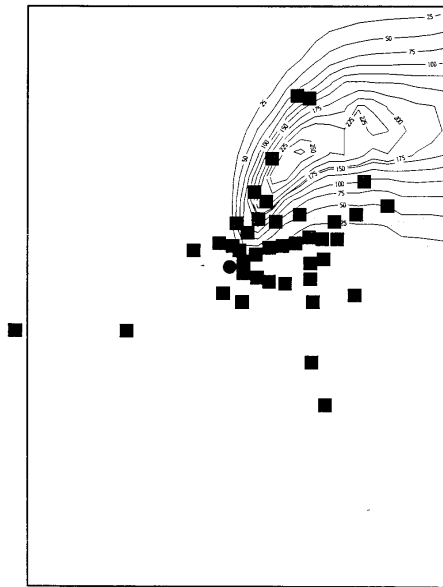the windfields in Fig. 2 a,b,c respectively (from: Martano, 1992)[12].

Figure 3c
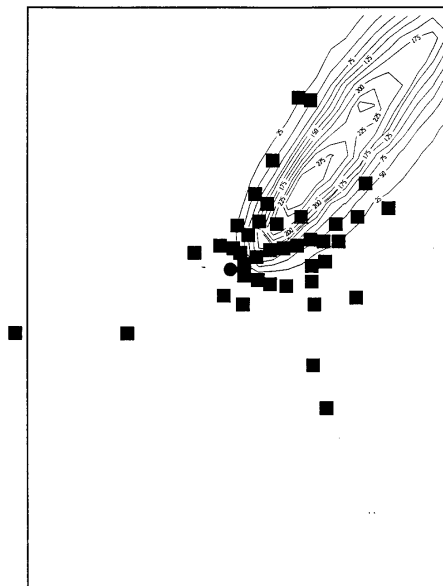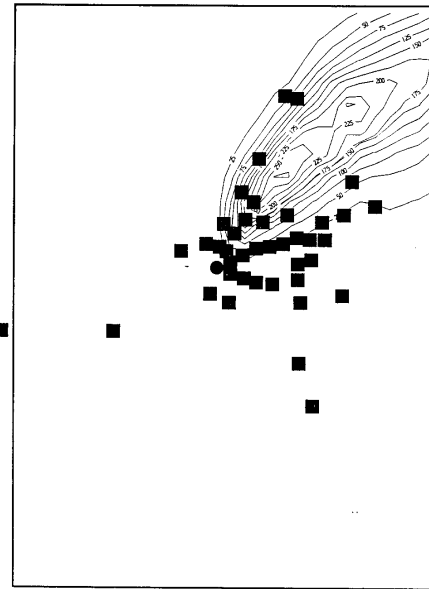
Figure 3. Surface concentration isopleths for EXP4 simulation in TIBL conditions. Squares indicate the location of the sampling points, and circles the location of the source (TA). The shape of the map is due to a standard graphic output of the model. a) Simulation with only experimental data. b) Simulation with only Flowstar data. c) All wind data simulation.

4. Analysis of the results: space variability and grid fields comparison

To better understand the model performances, as well as the differences between the used schemes of modelling, a standard set of statistical parameters has been used, that refers to the overall behaviour of the whole spatial distribution of surface concentrations, considered as a homogeneous statistical set (Hanna, 1988) [21].

This kind of analysis is then able to compare couples of statistical sets (such as model output and experimental data set, or couples of model outputs), establishing their degree of closeness, considering available spatial averages as for a given statistically homogeneous set, no matter which the representativity of each time-average in every sampling point due to its own fluctuation statistics. In other words: the statistics of sampling and averaging in a nonhomogeneous turbulence field is expected to vary with the location. This last problem involves in fact the point-by-point time behaviour of the turbulent fluctuations and will

Figure 3a

Figure 3b

be examined in the next section, where a kind of 'expected' uncertainty will be important for an 'intrinsic' comparison between model and experiment.

In turn, the aim of the present section is to establish statistical differences/closeness between spatial distributions of calculated or measured concentration averages, thus obtaining information about the relative degree of effectiveness of the different modelling schemes for the windfield and the atmospheric stability grids on the site. Then, the following parameters have been calculated with their statistical distribution, using a standard 'bootstrap' resampling procedure (Efron, 1982)[22], that avoids 'a priori' hypotheses about the (unknown) shape of the statistical distribution of the spatial concentration data sets, as suggested by Hanna (1988)[21].

Here the following averages $(< ... >)$ are intended to be calculated above the sample-points statistical set:

mean $= < C_e >$ or $< C_m >$ global experimental or modelled average

$sigma = < (C_e - < C_e >)^2 >^{1/2} = \sigma_e$ or

$< (C_m - < C_m >)^2 >^{1/2} = \sigma_m$ standard deviation

nmse $= < (C_m - C_e)^2 > /(< C_e > < C_m >)$ normalised mean square error

cor $= < (C_m - < C_m >)(C_e - < C_e >)/(\sigma_m \sigma_e)$ correlation coefficient

fa2 $=$ per cent of the sample-points in which $2 > C_e/C_m > 1/2$

fb $= 2 (< C_m > - < C_e >)/(< C_m > + < C_e >)$ fractional bias

fs $= 2(\sigma_m - \sigma_e)/(\sigma_m + \sigma_e)$ fractional bias of the standard deviations

The results of the parameters calculation is shown in Table I for different modelling schemes (wind/stability grids) of the experiments 2, 4 and 5 respectively (EXP2, EXP4, EXP5, from Martano, 1992)[12].

Table I - Rows Caption: 0: sampled experimental concentration set; 1: simulation with only 'Flowstar' wind data used; 2: same as 1, but in uniform neutral stability; 3: simulation with only experimental wind data used-, 4: same as 3, but in uniform neutral stability; 5: simulation with all available wind data used (in neutral stability for Exp5 only).

- **Exp2**								
model	mean	sigma	bias	mnse	cor	fa2	fb	fs
0	2.71	5.33	-	-	-	-	-	-
1	1.76	2.13	-.95	4.23	.603	.083	.423	.858
2	.63	.73	-2.08	17.26	.511	0	1.248	1.517
3	2.24	2.16	-.47	4.97	.139	.083	.189	.846
5	2.03	2.19	-.68	4.49	.389	.083	.288	.837
- **Exp4**								
model	mean	sigma	bias	mnse	cor	fa2	fb	fs
0	1.86	3.40	-	-	-	-	-	-
1	2.90	3.43	1.04	2.61	.442	.318	-.435	-.007
2	1.20	1.34	-.66	5.11	.262	.227	.432	.973
3	3.06	3.26	1.20	1.24	.748	.273	-.487	.043
4	1.40	1.72	-.47	3.80	.417	.318	.285	.659
5	2.79	3.17	.93	1.10	.778	.409	-.398	.072
- **Exp5**								
model	mean	sigma	bias	mnse	cor	fa2	fb	fs
0	.29	.39	-	-	-	-	-	-
1	.80	1.69	.51	10.79	.561	.176	-.929	-1.247
2	.37	.78	.08	2.61	.789	.235	-.236	-.658
3	.45	1.22	.16	10.35	.316	.235	-.430	-1.028
4	.15	.40	-.14	4.44	.414	.059	.616	-.009
5	.24	.54	-.05	2.50	.639	.235	.185	-.319

A glance to the above tables shows that a better compromise in terms of all the calculated parameters between measured and modelled concentration tends to be achieved when using wind grids coming from the extended wind data set (with the calculated wind profiles added).

More in detail, the (spatial) correlation parameter, being sensitive to the windfield changes, shows that in EXP2 and EXP5 the simulations 2 or 3, that use only experimental wind data, are very poor. Also in EXP4, simulations 1 or 2 with only calculated wind profiles fail in catching some essential features, but a best result is achieved when both experimental and calculated wind data are used (simulation 5).

This overall result is encouraging, as it seems to suggest that adding some calculated wind data to a too poor experimental set (one profile only) tends to better the performances of a mass-consistent reconstruction, no matter which reasonable locations are selected for the added data.

From the point of view of the stability grid, it appears that best overall results are obtained using the simulated TIBL conditions in EXP2 and EXP4, while only in EXP5 a homogeneous neutrality is more effective. The synoptic whether description from Biagio et al. (1985) [11] show that EXP5 corresponds to after-rain conditions in an overcast day.

It is important also to obtain an evaluation of the results from the point of view of the statistical significance of the differences between couples of models.

In Table II are shown the results of the calculated 'seductive' (i.e. from the 'bootstrap' distribution) 95% confidence interval for the differences in fractional bias between couples of models. Couples quoted for each of the three simulations correspond to those in which the calculated confidence interval for the fb parameter does NOT cross a vanishing value.

The mentioned couples are then those for which the parameter differences are statistically significant, and they clearly correspond to those in which the stability grid or both stability and windfield grid are different in all three simulations, while for EXP5 it is sufficient for only the windfield grids to be different.

Table II - Couples of concentration sets out of 95% confidence interval for the difference in fb.

Exp2	Exp4	Exp5
0-2	0-3	1-2
1-2	0-5	1-3
2-3	1-2	1-4
2-5	2-3	1-5
-	2-5	2-4
-	3-4	2-5
-	4-5	3-4
-	-	3-5
-	-	4-5

It is worth mentioning at this point that a direct simulation, strictly following the only available wind/stability information from the experimental data, would correspond to model 4 in EXP4 and EXP5. It is significantly different from the performance of model 5, resulting from a more detailed reconstructed meteorological information, enhanced in both vertical and horizontal spatial scale.

Concluding the present section: increasing the spatial resolution of the available meteorological data set appears then to be important for a better performance of a dispersion model in this complex coastal site.

5. Analysis of the results: time variability and uncertainty estimation

A point-by-point comparison between model results and monitored concentrations would require an estimate of the expected uncertainty of the latter.

That can be obtained from the three 20 minutes concentration averages which are available for each 1-hour dispersion experiment (Biagio et al., 1985)[11], where from a rough point-by-point estimate of the local variance of the time-averaged samples can be obtained.

As pointed out by Martano (1996b)[10], this discussion involves the comparison between statistical 'ensemble' averages (output of a K-diffusion model) and time averages (field-sampled concentrations). It is well-known (Papoulis, 1965, Tennekes-Lumley, 1972)[23,24] that the result depends on the ratio $R = T_c/T$ between averaging time T and correlation time scale T_c of the

concentration fluctuations at the given monitoring location, besides strictly requiring the statistical stationarity of the fluctuation field during the averaging time T to be meaningful.

Actually, if the fluctuation field can be considered stationary, that is $T_s >> T$, where T_s is the time scale of the 'boundary' conditions that determine the turbulence field on the site, then, in the hypothesis of an exponential self-correlation function with time scale T_c, it can be written:

$$< (C_T(x) - C_x)^2 >= 2\sigma_x^2 R(1 - R(1 - \exp(-1/R)))$$
$$(5.1)$$

where $C_T(x)$ indicates the T-averaged sample at x, C_x is the 'ensemble' ('true') average, σ_x^2 is the 'ensemble' ('true') variance, and $<>$ indicates here an 'ensemble' ('true statistical') average.

After estimating $< (C_T(x) - C_x)^2 >$ and σ_x^2, following Martano (1996b)[10], equation (5.1) can be used to give a point-by-point evaluation of T_c.

If R is small (typically $T/T_c >> 10$), the averages can be considered to have a gaussian distribution in view of the Central Limit Theorem, and then a student t variable can be constructed as:

$$t_x = n^{1/2}(C_e(x) - C_m(x)) \left[\sum_{i=1}^n \frac{(C_i(x) - C_e(x))^2}{n-1} \right]^{-1/2}$$
$$(5.2)$$

where $C_e(x)$ and $C_m(x)$ indicate respectively the experiment (1-hour) sample average and the model mean concentration at the point x, and $C_i(x)$ indicates each 20 minutes averaged value at the same point.

The null hypothesis is of course that the model mean represents the true statistical average concentration at the sampling point x.

If the above hypotheses were true for each sampling point, they all should have the same cumulative t distribution with $n-1$ degrees of freedom ($n = 3$: number of sampled concentrations in each receptor), say

$$P_x(t) = P(t, n - 1) \text{in each sampling point } x.$$

Then the cumulative experimental frequency $F_e(t_x) = n(t < t_x)/N$ can be plotted versus $P(t_x, 2)$ to test the above hypotheses ($n(t < t_x)$ = number of

sampling points with $t < t_x$, N = total number of sampling points).

The results for EXP2, EXP4, EXP5 are shown in Fig. 4 (from Martano, 1996b)[10], where the only data set that is close to the main diagonal corresponds to the experiment and simulation 4.
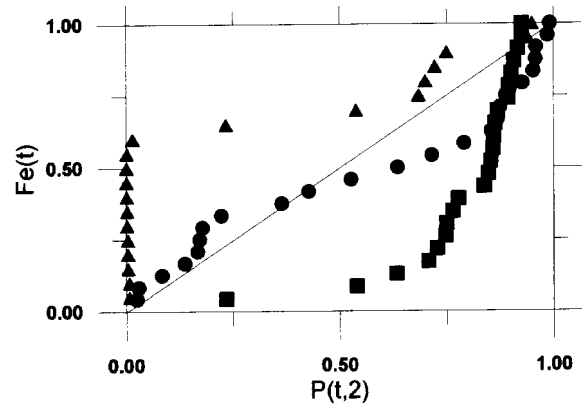

Figure 4. Experimental cumulative frequency Fo(t) versus Student t cumulative probability P(t,2): EXP2: triangles, EXP4: circles, EXP5: squares.

Table III shows the results of a Kolmogorov-Smirnov test for the maximum distance D between each of the three studied distribution and $P(t_x, 2)$. As expected only EXP4 gives a reasonable result for $P(d > D)$ being within a 90% confidence interval for the starting hypotheses (null hypothesis and gaussianity).

Table III. Results of the Kolmogorov-Smirnov test for $P(d)$, $d =$ maximum distance between $F_e(t)$ and $P(t, 2)$, D=actual value of d.

	EXP2	EXP4	EXP5
D	.58	.23	.53
$P(d > D)$	10^{-6}	.14	10^{-6}

The results of section 4, and the same modelling procedure used, do not seem to justify those strong differences, that could be related to the underlying local meteorological conditions during the experiments.

Table IV shows the results of a simple linear trend detection applied to the time series of some meteorological/turbulence parameters P obtained from the measured data during the three experiments: the measured wind speed at 100 m height at TA V(100m), and the

surface values of the velocity and temperature turbulent fluxes, $< uw >$ and $< w\theta >$, obtained from the vertical wind/temperature gradients of the tower data at TA (Martano, 1996b).

Table IV. Stationarity estimators for the local meteorological parameters p: a = slope of the time trend ($p = at + b$), r = linear regression coefficient.

		EXP2	EXP4	EXP5
P=V(100m)	a	$-.36 \pm .06$	$-.06 \pm 3$	$.91 \pm .22$
	r	-.91	-.10	.86
P=<uw>	a	$-.02 \pm .001$	$.003 \pm .008$	-
	r	-.51	.14	-
P=< $w\theta$ >	a	-3.4 ± 1.4	$.28 \pm 2.2$	-
	r	-.68	.05	-

It appears that a time trend exists in the local meteorological conditions for both EXP2 and EXP5, but that is absent in EXP4. Thus, the lack of statistical significance, in apparently non-stationary environmental conditions, for both the 1-hour averaged sampled concentrations as well as for the averaged meteorological input data used in he simulations, can be an explanation for the failure of the comparison in the case of EXP2 and EXP5.

Closely following the time evolution of the local meteorology appears then to be another strong requirement in simulating atmospheric dispersion in this coastal site, although a warning must be considered: the short time scale of the meteorological variability along the coastline can make difficult a comparison between model results and sampled concentration data.

Discussion and conclusions

The performed statistical analysis confirms the ideas about modelling atmospheric dispersion in complex coastal sites that were outlined in the introduction.

The comparison of the spatial concentration distributions obtained as model outputs showed that results get generally closer to the monitored concentration data when the spatial resolution of the input data that define the local meteorology is increased.

Moreover, if experimental data are available only in one or few locations over a complex topography, the results of constructing wind/stability grid above this poor initial data set is worse than that obtained with the aid of 'artificial' data coming from approximate physical models. This is true when simple interpolative or

mass-consistent model are used, that can be interpreted as follows: a topographic variability scale too smaller than the resolution of the data set causes an error that is greater then that caused by artificially increasing the initial spatial resolution through calculated data.

Similar results hold for the time variability. It is seen that time trends in the local meteorology in scales of the order of one hour can be frequent in coastal sites, and can invalidate the use of static grids for wind-field/turbulence for integration times as short as one hour.

More dramatic: the short time variability can conflict with the local turbulent fluctuation time scale, in the sense that the inequality $T_s >> T >> T_c >$ that is necessary for a statistically significant comparison between model output and field-averaged concentrations, can fail to hold if T_c and T_s differ for less than two orders of magnitude. Indeed it has been estimated (Martano, 1996b)[10] that the correlation time scale T_c of the concentration fluctuations could be of several replace tens of seconds in particular conditions, which could affect the basis of the usual statistical data analysis if T_s is too short (less than one hour). This could make difficult a proper assessment of the model performances if the meteorological conditions during the experimental campaign are subject to too quick variations.

Eventually, some suggestions about a real-time modelling of the atmospheric dispersion in the Angra site can be obtained:

1) The spatial resolution of the meteorological information about wind and surface fluxes must be enhanced increasing the number of sampling points (meteorological towers and surface stations) to cover all the key points of the topography of the site and enhance the vertical resolution. The wind/turbulence grids used in modelling should always take into account data coming from all available location.

2) The time evolution of the wind/turbulence grid must be thoroughly taken into account and the used grids must be replaced by the new ones in time steps of fractions of one hour, following the new available meteorological data set. Thus the dispersion model must be able to work over grids that are changing with a quite short time step. Puff release models or lagrangian particle models (Zannetti, 1990)[24] could then be used, provided the former to follow the vertical inhomogeneity of the fields ('skewed puffs') and the latter to be fast

enough to achieve a reasonable statistics in only several minutes of runtime.

3) Any attempt to validate a model over field measurements on the site should take into account explicitly the stationarity of the meteorological conditions during the averaging/simulation time.

Acknowledgements

References

1. Lalas D.P., Ratto C.F.: *Modelling of atmospheric flow fields.* World Scientific Publishing, Singapore, 1996,

2. Sasaki Y., 1958: An objective analysis based on the variational method.- J. of the Met. Soc. of Japan, **36**, pp.77-88.

3. Jackson P.S., Hunt J.C.R., 1975: Turbulent wind flow over a low hill. - Q. J. R. Met Soc., **11**, pp.833-851.

4. Raynor G.S., Brown M.P., Sethu Raman S., 1975: Studies of atmospheric diffusion from a nearshore oceanic site - J. of Appl. Met. **14**, pp. 1080-1094.

5. Lyons W.A., 1976: Turbulent diffusion and pollutant transport in shoreline environrnents.- In 'Lectures on air pollution and environmental impact analyses', A.M. S., Boston, pp.136-208.

6. Brutsaert W., 1982: *Evaporation into the Atmosphere.* - Kluwer Acad. Publ., Dordrecht.

7. Atkinson B.W. Press, *Meso-scale Atmospheric Circulations.* Academic Press, 1981.

8. Martano P., 1996a: Detection of mesoscale-driven circulations from time series of wind speed. Nuovo Cimento C, vol. **19** n. 4, pp. 579-590.

9. Hastenrath S.: *Climate dynamics of the tropics.* Ed. Kluwer Acad. Publ., 1991.

10. Martano P., 1996b: Coastal environment and statistical uncertainty in atmospheric dispersion modelling. A case study in Brazil. In: Coastal Environment - Environmental problems in coastal regions, A.J. Ferrante and C.A.Brebbia editors, Computational Mechanics Publ., 1996, pp. 239-248.

11. Biagio R., Godoy G., Nicoli I., Nicolli D., Thomas P., 1985: First atmospheric diffusion experiment campaign at the Angra site. - KfK 3936, Karlsruhe, and CNEN 1201, Rio de Janeiro.

12. Martano P., 1992: Dinâmica de fluxo turbulento sobre relevo e aplicação à difusão em pequena escala na camada limite atmosférica. Tese de doutorado, P.U.C., Dep. de Física, Rio de Janeiro.

13. Martano P., Tampieri F., Busuoli M., Zanini G., 1991: Application of wind models on the local scale by means of standard meteorological data.- Annals of VII Brazilian Congress of Meteorology, vol.2 pp.585-560, S. Paulo, Brazil, 1992

14. Busuoli M., Zanini G., l991a: ATMOSl, manuale d'uso. ENEA, Bologna.

15. Carruthers D.J., Hunt J.C.R., Weng W.S., 1988: A computational model of stratified turbulent air flow over hills: FLOWSTAR I. Proceedings ENVIROSOFT, Computer Techniques in Proceedings of: Environmental Studies', P. Zannetti ed., Springer Verlag, erlm, pp.481-492.

16. Hunt J.C.R, Leibovich S., Richards K.J.,1988: Turbulent shear flows over low hills.- Q.J. R. Met. Soc. **114**, pp.1435-1470.

17. Busuoli M., Zanini G., l991b: ATMOS2, manuale d'uso. ENEA, Bologna.

18. Smith T.B., Howard S.M., 1972: Methodology for treating diffusivity. - Informal Report MRI 72 FR-1030, Met. Research Inc.

19. Taylor R.J., Warner j., Bacon N.E., 1970: Scale length in atmospheric turbulence as measured from an aircraft.- Q.J.R. Met. Soc. **96**, pp. 750-755.

20. Stunder M., Sethu Raman S.,1984: A comparative evaluation of the coastal internal boundary layer height equations. Boundary Layer Meteorol., **32**, pp. 177-204.

21. Hanna S.R., 1988: Air quality model evaluation and uncertainty. J.A.P.C.A., **38**, pp. 406-412.

22. Efron B., 1982: The Jacknife, the Bootstrap, and other resampling plans.- CBMSS-NSF-38, Society for Industrial and Applied Math. Philadelphia.

23. Papoulis A.: *Probability, Random Variables and Stochastic Processes.* McGraw-Hill, New York, 1965.

24. Tennekes H., Lumley J.L.: *A first Course in Turbulence.* MIT Press, Cambridge, 1972.

25. Zannetti P., 1990: *Air Pollution Modeling.* - Ed. Computational Mechanics Publications.